JOURNAL OF MATERIALS SCIENCE 11 (1976) 510–521

# Superplastic deformation of the Pb-Sn eutectic

A. E. GECKINLI, C. R. BARRETT
*Department of Materials Science and Engineering, Stanford University, Stanford, California, USA*

Dynamic observations of grain-boundary sliding during superplastic flow of the Pb–Sn eutectic are reported. These observations confirm the postulate that the dominant deformation mode during superplastic flow is grain-boundary sliding with localized deformation necessary to maintain grain coherency. Extensive grain-boundary sliding is also observed when the strain-rate and/or grain size is outside the superplastic flow regime. Stress relaxation tests were also carried out on the Pb–Sn eutectic. These tests provide data on the activation energy ($45 \pm 5\,kJ\,mol^{-1}$), grain-size dependence ($d^{-3}$), and stress dependence of superplastic flow in this alloy. A threshold stress of $1.3 \times 10^6\,N\,m^{-2}$ for the onset of superplastic deformation is also observed.

## 1. Introduction

Superplastic flow in metals is characterized by extremely large plastic extensions (up to 2000%) prior to fracture. Two necessary prerequisites for observance of superplasticity are a testing temperature greater than half the absolute melting temperature, so that diffusional processes occur rapidly, and a small equi-axed grain size, usually less than $10\,\mu m$. Grain sizes this small generally cannot be maintained in single phase alloys at high temperatures and correspondingly superplasticity is usually observed in two phase materials often with eutectic or eutectoid composition. The characteristic microstructural feature of superplastic deformation is the retention of the equi-axed grain structure throughout deformation. This observation, coupled with a review of other pertinent data on superplasticity (see review papers by Davies *et al.* [1], Johnson [2] and Nicholson [3]) has led to the conclusion that grain-boundary sliding is the dominant deformation mechanism during superplastic flow.

The simple physical picture of superplastic deformation that has been built up can be described with reference to the geological analogy suggested by Gifkins [4]. In this analogy each grain is divided into a central "core" and a "mantle" which is the grain-boundary region. Grain-boundary sliding can lead to large strains with no disturbance of the core if the incompatibilities developed at the grain boundaries are relieved by deformation on the mantle. The deformation of the mantle changes in sign and magnitude depending on the local surroundings of the grain and on average leads to no net change in grain shape.

Preliminary dynamic observations of grain-shape changes during superplastic flow by Dingley [5] and Geckinli *et al.* [6] substantiate this simple model. These studies, which are observations of surface grain topography, show grains to readily slide past their neighbours with only minor grain-shape changes. Although the generality of these observations may be questioned because the results are from surface grains, where local constraint by adjacent grains is different from the interior of the sample, the results are consistent with data obtained from internal observations. That is, in both instances the equi-axed grain shape is preserved and there is no evidence of recrystallization. The only deformation processes observed are grain-boundary sliding and local grain deformation near the grain boundaries to maintain grain coherency. Thus it appears likely that these dynamic observations are indicative of the actual deformation process.

The purpose of the present paper is to report more detailed observations on relative grain motion during superplastic flow. As in the earlier studies [5, 6], samples of the Pb–Sn eutectic composition were deformed in a scanning electron microscope and the surface grain topography was continuously recorded during deformation. The study concentrated on the influence of grain size, strain-rate, and the presence of a finely distributed third phase on the superplastic flow properties.

An additional aspect of the present study concerns the proposed model that the dominant deformation mode is grain-boundary sliding coupled with localized grain deformation to maintain grain coherency. In terms of macroscopic deformation kinetics, this model predicts that there should be a threshold stress for plastic deformation and also a variable strain-rate sensitivity throughout the superplastic flow region [7, 8]. The latter feature is commonly observed, whereas the former, which should occur at low strain-rates, has been reported only a few times [9–11]. In view of the scarcity of data on the existence of a threshold stress for superplastic flow, the present investigation also documented the deformation kinetics of the Pb–Sn eutectic alloy over a wide range of test conditions (grain size, strain-rate, and test temperature). It was hoped that such a study would clearly document the low strain-rate range of the superplastic deformation region and provide additional information as to the nature of the rate controlling deformation process.

## 2. Experimental procedure

The Pb–Sn eutectic alloy was prepared from 99.99% Pb and 99.99% Sn by melting and casting in air. The microstructure of the cast alloy was a typical eutectic structure with a lamellar spacing of approximately 1.5 $\mu$m. The lamellar structure was changed to an equi-axed structure by rolling at room temperature with a maximum reduction of 5% per pass. The rolling process took approximately 2000 sec after which the rolled sheets were stored at 258 K. The grain size immediately after rolling was approximately 1.5 $\mu$m. Larger grain sizes were prepared by annealing at temperatures up to 423 K.

A precipitation hardened Pb–Sn eutectic alloy was also prepared for study. This alloy was melted as above with the addition of 0.1% of 99.99% Au. The alloy was water quenched to 20° C to form a supersaturated solid solution. Replica electron micrographs showed that ageing at 423 K for $2.5 \times 10^5$ sec produced a uniform distribution of $AuSn_4$ precipitates which were approximately $10^{-2}$ $\mu$m in diameter with an average spacing of $10^{-1}$ $\mu$m. The aged alloy was cold-rolled and annealed as in the case of the pure Pb–Sn eutectic to produce a fine grained equi-axed structure. Further replica studies showed that the precipitate size and distribution did not change during the rolling and annealing process.

Dynamic observations of grain-shape changes during superplastic flow were carried out using a specially designed tensile stage in an AMR 900 scanning electron microscope. The tensile stage, shown in Fig. 1, was designed such that the ends of the sample are translated in opposite directions at equal velocities. This allows the centre of the sample to remain essentially motionless and greatly facilitates continual observation of one area on the surface at high magnification (1000 to 10 000 ×). Surface structure was recorded continuously using a cine camera or using normal photographic procedures and stopping the deformation whenever it was desired to take a photograph. Tests have shown that such interruptions in the tensile test have no observable effect on the subsequent deformation characteristics. The test procedure was essentially one of constant cross-head speed rather than constant strain-rate. Tests were carried out for sample with different grain size (3 to 10 $\mu$m) tested at room temperature ($T/T_m = 0.65$) in the strain-rate range of $5 \times 10^{-4}$ to $5 \times 10^{-3}$ sec$^{-1}$.

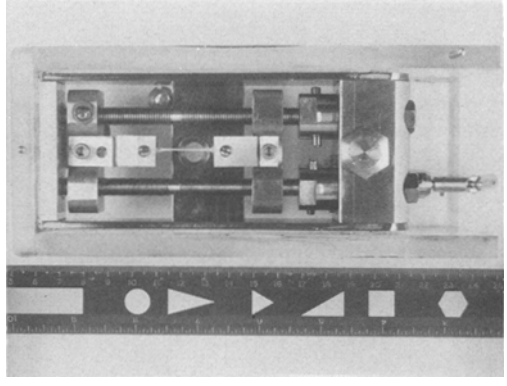

*Figure 1* The miniature tensile stage used for scanning electron microscope observations. An elongated tensile sample is in place.

Miniature tensile specimens for the scanning microscope tensile stage were cut from the rolled sheet material using electro-spark machining. The gauge section of the tensile samples was 3 mm long,

1.7 mm wide and 0.5 mm thick. The rolling direction was parallel to the tensile axis. Grain size determinations were made from scanning electron micrographs of slightly ($\approx 1\%$ strain) deformed specimens by counting the number of intersections of grain boundaries with randomly oriented lines. No less than 400 intersections were counted for each determination.

Mechanical testing to determine macroscopic flow kinetics was carried out using the stress relaxation technique described by Lee and Hart [12]. The advantage of the stress relaxation method is the large range of strain-rate that can be studied in a single relaxation. In this study, where interest was focused on the low strain-rate (low stress) region of the stress–strain-rate relation, particular attention was given to long time relaxation tests. The total relaxation time was usually between $4 \times 10^4$ and $10^5$ sec depending on the specimen grain size and test temperature. To minimize the effects of grain growth during testing, specimens with a grain size below 3 $\mu$m were not tested.

Tests were performed at different temperatures in the range 263 to 353 K. For temperatures below room temperature a liquid-nitrogen cooled ethyl alcohol bath was used. For temperatures in the range 298 to 323 K a hot water bath was used and for temperatures higher than 323 K a resistance heated furnace was employed. All the specimens were held 1800 sec at test temperature before the testing. To minimize temperature changes during the low temperature relaxation tests, relaxations were terminated after about 1200 sec. Temperature control during the course of the relaxations was better than 0.5 K.

For the stress relaxation tests, specimens were first deformed in tension until the maximum flow stress was attained. The cross-head motion was then stopped and the unloading characteristics recorded. The total plastic strain before the relaxation was between 0.02 and 0.07. The unloading rate ($dP/dt$) at any time $t$, during the relaxation was obtained by measuring the slope along the load–time record.

The general relation between the strain-rate $\dot{\epsilon}$ and the unloading rate $dP/dt$ is as given by Lee and Hart [12] where

$$\dot{\epsilon} = -\frac{1}{K_{\text{total}}\left(L_0 + x - \frac{P}{K_{\text{total}}}\right)}\left(\frac{dP}{dt}\right) \quad (1)$$

with $K_{\text{total}}$ the elastic constant of system (machine and specimen), $x$ the cross-head displacement measured from the start of the test to the beginning of the stress relaxation, $P$ the load, and $L_0$ the initial gauge length of the specimen ($3.8 \times 10^{-2}$ m). Since the $P/K_{\text{total}}$ term is always small, it can be neglected.

Taking $L_1 = L_0 + x$, Equation 1 can be rewritten

$$\dot{\epsilon} = -\frac{1}{K_{\text{total}} L_1}\left(\frac{dP}{dt}\right). \quad (2)$$

This relationship indicates a simple proportionality between the strain-rate ($\dot{\epsilon}$) and the unloading rate ($dP/dt$). The proportionality constant is easily evaluated as the initial loading portion of the test gives a measure of the elastic constant $K_{\text{total}}$ and $L_1$ is merely equal to the specimen length just before the relaxation. Since it is possible to measure ($dP/dt$) from the relaxation curves, $\dot{\epsilon}$ versus stress data can be obtained directly from Equation 2.

It should be pointed out that determination of $K_{\text{total}}$ can involve some error. For superplastic materials or, in general, for any high temperature deformation, the initial loading portion of the stress–strain curve may be associated with some plastic deformation. However, even if there is some error in determining $K_{\text{total}}$ this does not introduce any error in the shape of the $\dot{\epsilon}$–$\sigma$ curves, only the absolute magnitude of the strain-rate may be slightly in error. In this paper to avoid this problem, the stress relaxation data are presented in terms of ($dP/dt$) rather than $\dot{\epsilon}$. A typical value for $K_{\text{total}}$ is $1.13 \times 10^6$ N m$^{-1}$. Using this value of $K_{\text{total}}$ the reported relaxation rates can be converted to strain-rates by dividing by $4.3 \times 10^{-4}$ N.

The minimum value of stress for which the present stress relaxation data are considered valid is about $5 \times 10^5$ N m$^{-2}$. Below this stress level, sample linkage weight and a variable machine elastic constant make an accurate determination of $K_{\text{total}}$ impossible.

## 3. Results

We first consider the influence of grain size, strain-rate, and precipitate presence on relative grain motion during superplastic flow and then examine the deformation kinetics of he Pb–Sn eutectic alloy.

### 3.1. Observations for small grain size samples

In this section data are reported for samples with a grain size in the range 3 to 4 $\mu$m. The majority of

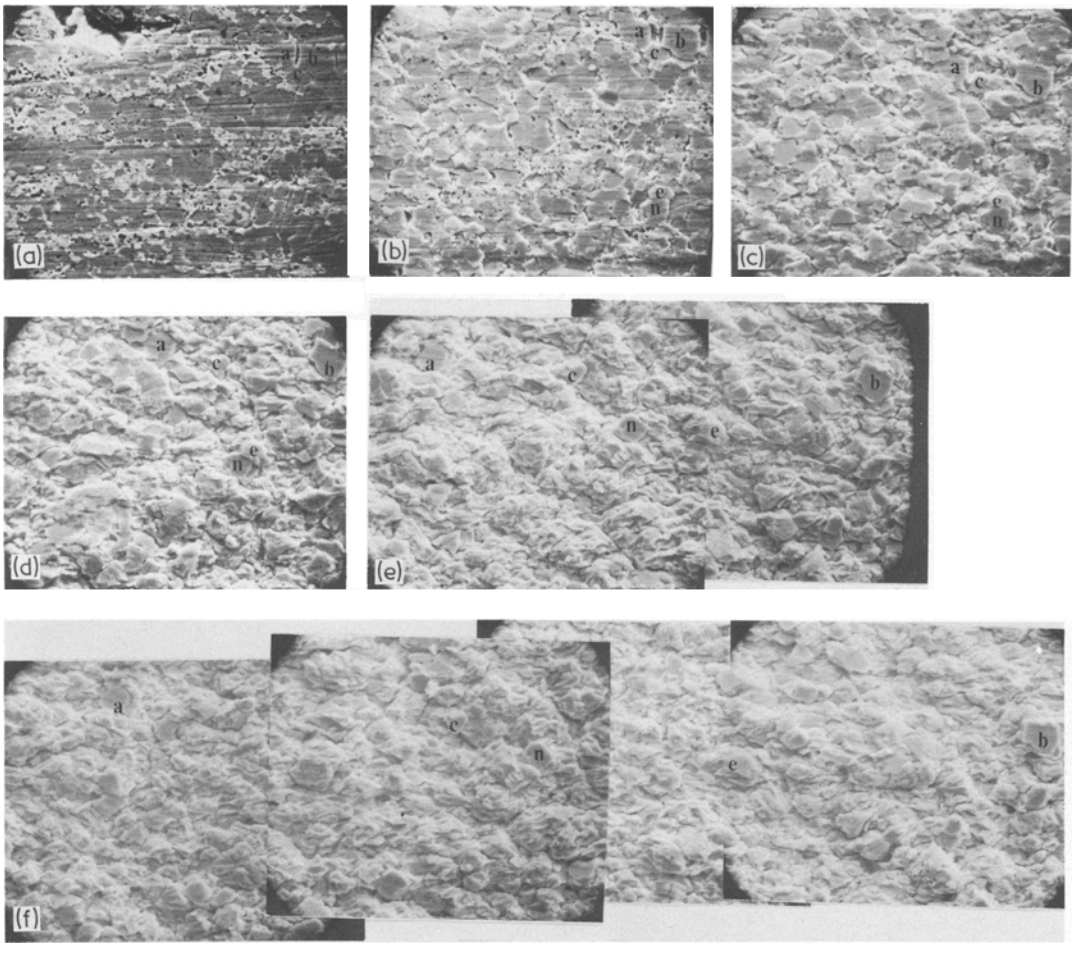


*Figure 2* Relative motion of surface grains in Pb–Sn eutectic alloy tested at 298 K and at an initial strain-rate of $5 \times 10^{-4}$ sec$^{-1}$. Tensile axis is horizontal. Grain size is equal to 3.5 $\mu$m. Elongation: (a) 6.65%; (b) 25.8%; (c) 87%; (d) 182%; (e) 365%. (f) 500%.

the observations are on samples deformed under superplastic flow conditions, although some comparative observations are reported at strain-rates above the superplastic regime. Elongations of 300 to 500% were observed in the superplastic strain-rate range of 5 to $10 \times 10^{-4}$sec$^{-1}$. A portion of a typical set of micrographs for a sample deformed in the scanning electron microscope is shown in Fig. 2. Normally photographs were taken every 15 to 20% strain. Features of the deformation process evident from this set of micrographs and other similar tests include the following.

*Grain-boundary sliding:* grain-boundary sliding occurs to a large extent, and two initially adjacent grains may end up many grain diameters apart (follow grains a, b and c in Fig. 2). The relative motion of two initially, adjacent grains depends on the resolved shear stress across the grain interface with grains with transverse or longitudinal boundaries generally moving apart less rapidly than other grain orientations. This observation is obviously complicated by the planar nature of the surface observations as only the surface trace angle of the grain boundary is observed.

Grain-boundary sliding is observed at the onset of plastic flow and small apparent gaps are developed between surface grains at low strains due to sliding. After about 20% strain new grains began to emerge to the surface from the interior to fill the gaps. This basic process continues throughout the strain range investigated. Most surface grains present at large strains were initially located in the specimen interior. The original surface grains are readily recognizable because of their flat facets (polished surface) whereas the previously interior grains are more rounded in character.

*Constancy of grain shape:* it is observed that

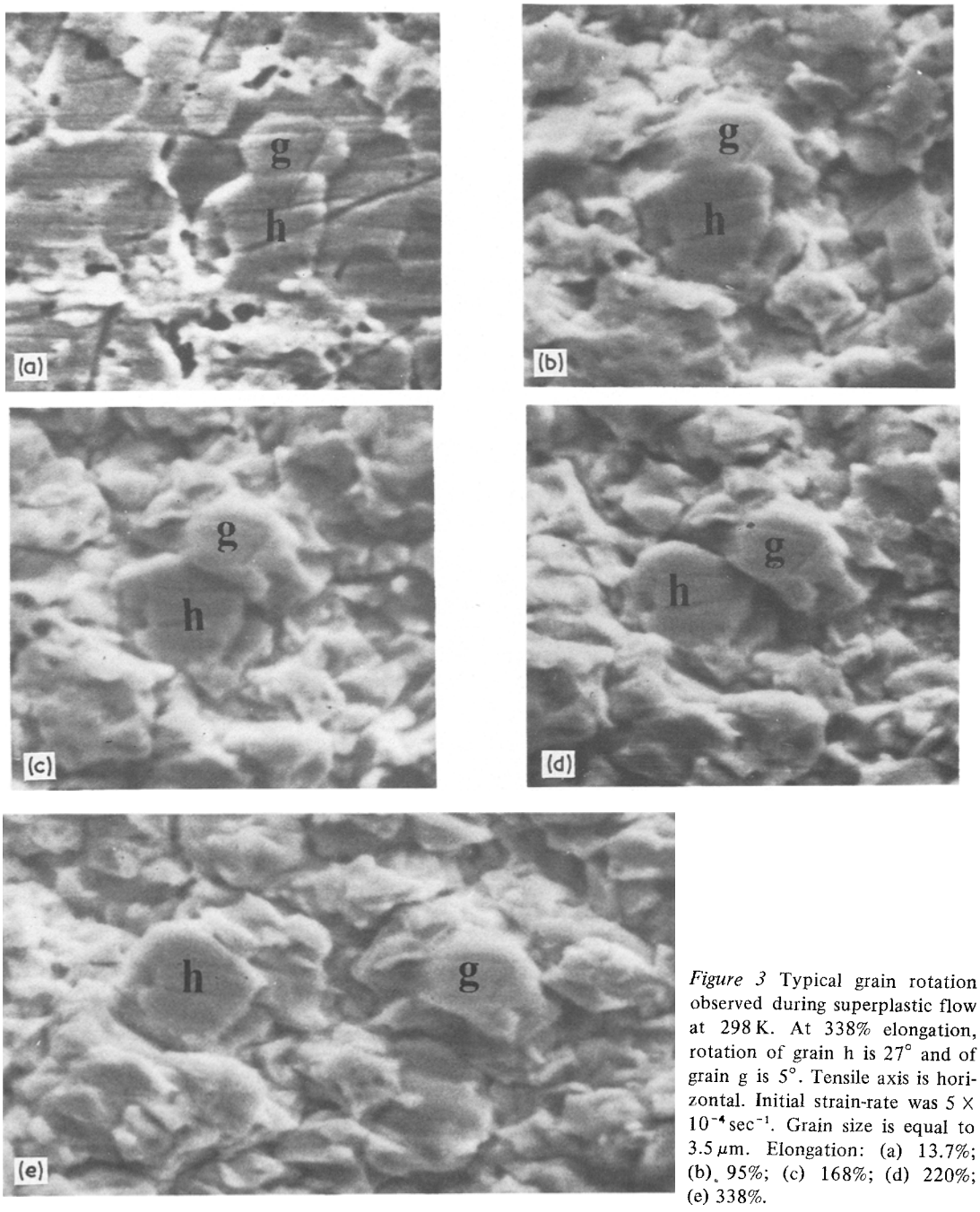


*Figure 3* Typical grain rotation observed during superplastic flow at 298 K. At 338% elongation, rotation of grain h is 27° and of grain g is 5°. Tensile axis is horizontal. Initial strain-rate was $5 \times 10^{-4}\,sec^{-1}$. Grain size is equal to 3.5 $\mu$m. Elongation: (a) 13.7%; (b) 95%; (c) 168%; (d) 220%; (e) 338%.

grains maintain approximately their original shape during superplastic flow. There is never any gross change in shape. The only evidence of grain deformation is near the grain boundaries. After deformation, grain boundaries become curved. Interior grains that appear at the surface also show this localized deformation. During superplastic flow grains do not elongate in the direction of tensile axis. The magnitude of localized strains (grain-shape change) was estimated from surface observations to be less than a few percent.

No attempt was made to compute the contribution of grain-boundary sliding to the total strain by measuring offsets across grain boundaries because each grain generally had several different neighbours during the course of any one test. Instead, the observations that on average grains move apart at a rate commensurate with the imposed strain-rate and grain shape is essentially constant were taken as evidence that grain-boundary sliding accounted for nearly all the strain.

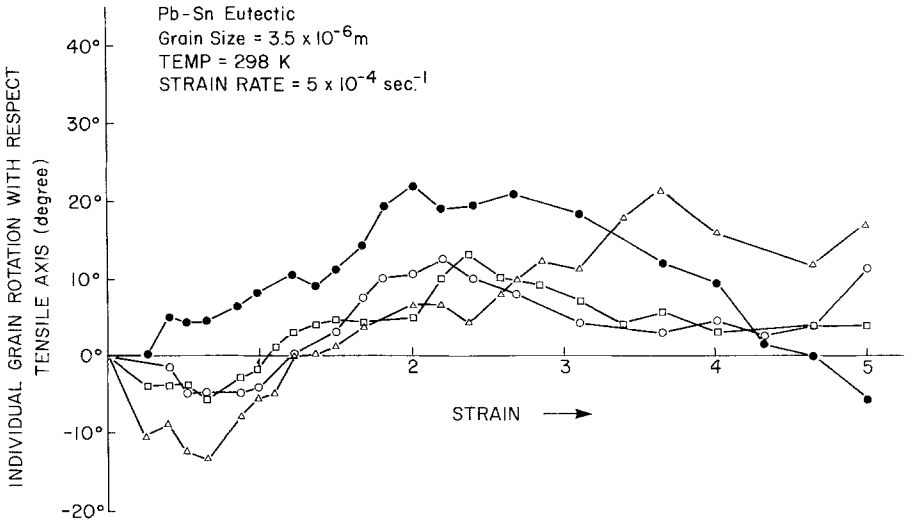


*Figure 4* Grain rotation during superplastic flow at 298 K. Initial strain-rate was $5 \times 10^{-4}\,sec^{-1}$. Grain size is equal to 3.5 $\mu$m.

*Rotation of grains:* individual grains are observed to rotate appreciably during superplastic flow. A typical example is shown in Fig. 3. The amount of rotation varies from grain to grain although generally rotations less than $\pm 30^{\circ}$ are observed. The rotation of any single grain often changes sign during the course of any one test, indicating that the sense of rotation for one grain depends sensitively on its instantaneous surroundings (see Fig. 4). These data suggest that grain rotation accompanies grain-boundary sliding giving additional freedom with which to maintain coherency. There is no evidence that grain rotation is responsible for maintaining the equi-axed grain shape during superplastic deformation as proposed earlier [13].

*Void formation:* no void formation is observed at the surface during superplastic flow except for the small gaps developed due to grain-boundary sliding at the early stages of deformation. These gaps or microcavities are readily filled by subsurface grains as deformation continues. If the strain-rate is increased above the superplastic range fewer subsurface grains appear and the grain-boundary gaps grow to form cracks between surface grains as they move apart. This is shown in Fig. 5 (cf. Fig. 2 for same strain). The growth of these cracks is observed to cause ultimate failure.

An attempt was made to determine if microcavities also exist in the interior of the sample during superplastic deformation. Normal metallographic techniques did not reveal any cavities and thus an alternative, less direct technique was

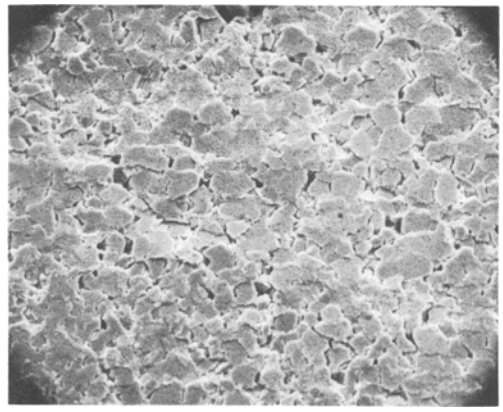

*Figure 5* Cavity formation due to grain-boundary sliding at high strain rates. Elongation is 25%. Tensile axis is horizontal. Initial strain-rate was $2 \times 10^{-3}\,sec^{-1}$. Grain size is equal to 3.6 $\mu$m.

employed. Two samples, one deformed 35% under superplastic conditions and one undeformed, were fractured at liquid nitrogen temperature. The fracture surfaces were then examined for evidence of pre-existing voids. The fracture surfaces are shown in Fig. 6. The undeformed sample shows an intergranular fracture mode with some ductile tearing in the Pb-rich phase. The deformed sample exhibits considerably more evidence of dimpled rupture failure with numerous areas where the dimple spacing is much smaller than the grain size. This difference in fracture mode is suggestive that small voids (or void initiation sites) are generated during superplastic flow. If these voids exist they apparently do not continually grow during superplastic deformation. If it were otherwise, then

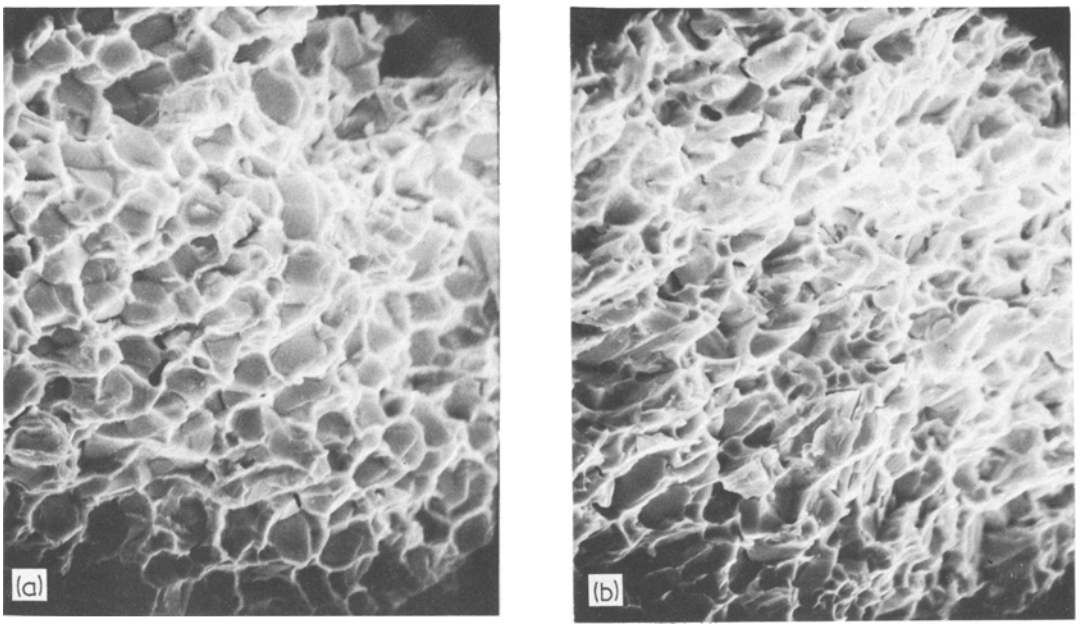


*Figure 6* Fracture surfaces of (a) undeformed and (b) superplastically deformed 35% Pb–Sn eutectic fractured at 77 K. Superplastic deformation rate was $4.6 \times 10^{-4}\,sec^{-1}$. Grain size is equal to 3.1 $\mu$m.

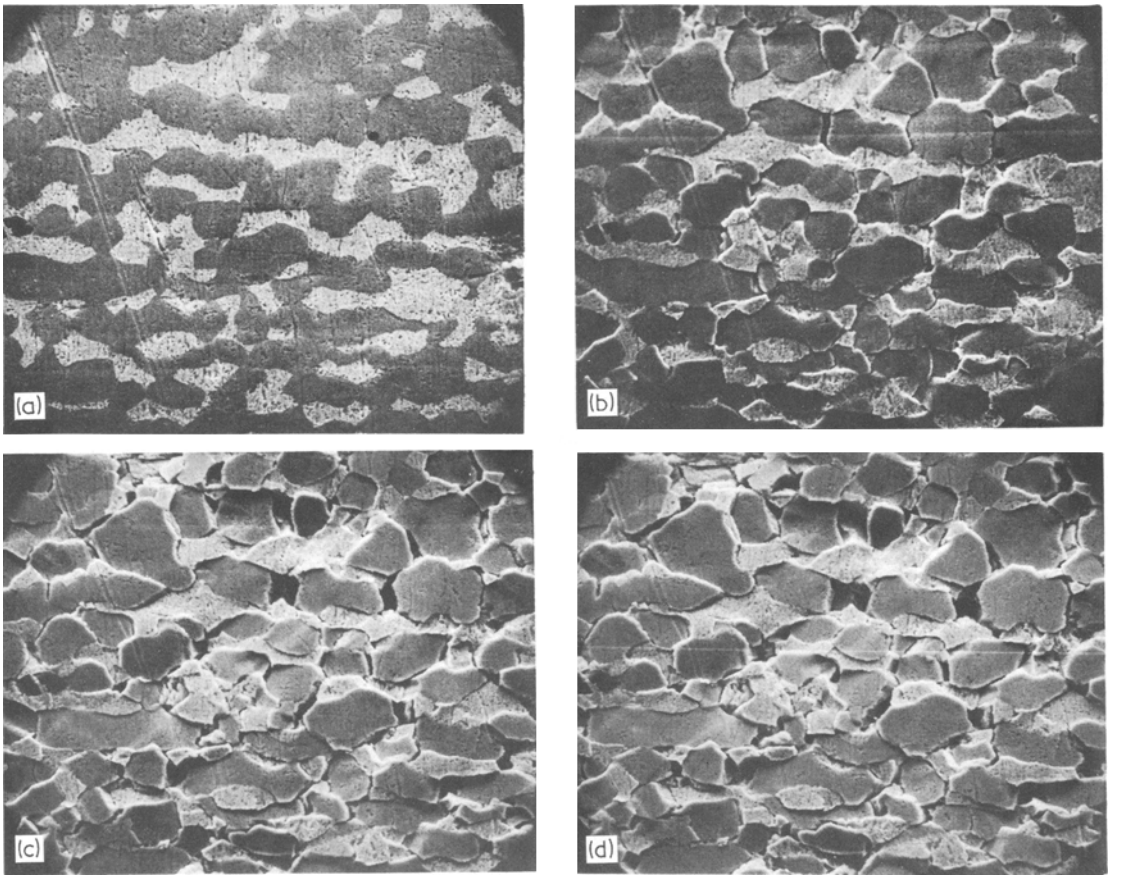


*Figure 7* Relative motion of surface grains in Pb–Sn eutectic alloy tested at 298 K and at an initial strain-rate of $5.4 \times 10^{-4}\,sec^{-1}$. Tensile axis is horizontal. Grain size is equal to 9.5 $\mu$m. The dark phase is tin-rich. Elongation: (a) 0%; (b) 8.9%; (c) 20.2%; (d) 41%.

void growth and coalescence would cause fracture before superplastic elongations occurred. It may be that voids alternatively grow and shrink during superplastic flow as grains continually slide past one another.

*Other observations:* no recrystallization or slip-bands were observed during superplastic flow. Scratches on individual grains remained sharp and equally spaced throughout the entire deformation process.

### 3.2. Observations for large grain size samples

Superplasticity was not observed for grain sizes greater than 4 $\mu$m when tested in the scanning microscope in the strain-rate range 5 to $10 \times 10^{-4}$ $sec^{-1}$. Total elongation to fracture was observed to be 30 to 60% compared with 300 to 500% for fine grained samples tested in the same strain-rate range.

Fig. 7 shows a typical series of surface observations for a large grain size specimen. The features evident in this series of micrographs and other similar tests can be summarized as follows. The early stages of deformation involve extensive grain-boundary sliding as in the case of fine grained specimens. However, subsurface grains rarely emerge to the surface from the interior. Instead, sharp, angular shaped voids form between grains due to the incompatibility developed during grain-boundary sliding. These voids coalesce and ultimately cause failure.

During deformation the grains do undergo measurable shape changes. Estimates of the contribution of grain deformation to the total elongation suggest that grain deformation contributes 20 to 50% of the total strain.* The remainder of the strain is due to voids, or grain-boundary sliding, as for the large grain sizes nearly all grain-boundary sliding results in void formation.

In summary, grain-boundary sliding is the main deformation mode for both small and large grain sizes in the size range investigated. Small grain sizes show extensive grain-boundary sliding where a single grain may have many different neighbouring grains during superplastic flow. Little void formation is observed. For large grain sizes there is little accommodation of grain-boundary sliding, voids form early in the deformation and fracture results. Thus the main difference between the deformation of small and large grain size samples is not so much the occurrence of different deformation modes but rather a difference in the efficiency of the accommodation process which accompanies grain-boundary sliding.

### 3.3. Influence of precipitate distribution on superplastic flow

Accommodation to maintain grain coherency during grain-boundary sliding can occur by either directed vacancy diffusion or dislocation motion.

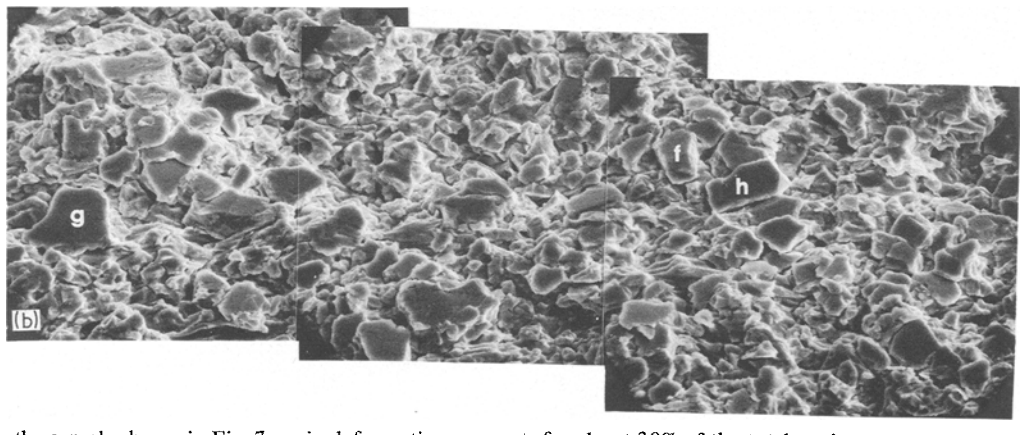


*Figure 8* Relative motion of surface grains in Pb–Sn eutectic containing a fine dispersion of $AuSn_4$ and tested at 298 K. Tensile axis is horizontal. Initial strain-rate was $5 \times 10^{-4}$ $sec^{-1}$. Grain size is equal to 3.5 $\mu$m. Elongation: (a) 12.7%; (b) 124%.

* For the sample shown in Fig. 7, grain deformation accounts for about 30% of the total strain.

Whichever process occurs most likely controls the rate of boundary sliding and hence the overall strain-rate during superplastic flow.

If accommodation occurs by diffusional creep, the presence of a finely dispersed precipitate phase should have little effect on superplastic properties. On the other hand, if accommodation occurs by dislocation motion the superplastic properties are expected to be significantly effected. That is, if dislocation motion is impeded by precipitates and grains can no longer maintain coherency then voids are nucleated and grow with the consequence that superplasticity is lost.

Samples containing a fine dispersion of $AuSn_4$ in the Pb–Sn eutectic structure were deformed in the scanning electron microscope. A portion of a typical set of micrographs is shown in Fig. 8. Observations of grain-boundary sliding and grain translation show deformation characteristics identical to those for the small grained eutectic alloy without precipitates. Whereas these observations suggest the precipitate distribution has no effect on the deformation process it should be noted that the total elongation of the Pb–Sn–Au alloys was about 150% compared to 300 to 500% for Pb–Sn in the superplastic region. This may be due to the $AuSn_4$ particles acting as void initiation sites at grain boundaries or some slight restriction in the accommodation process. Regardless of the exact mechanism, the extensive grain-boundary sliding observed suggests that the majority of grain accommodation occurs via diffusional creep and not dislocation motion.

## 3.4. Deformation kinetics

The data obtained from the stress relaxation tests are shown in Fig. 9. These results can be conveniently divided into two main regions. The low stress region, where the data suggest the strain-rate sensitivity $m = (\mathrm{d} \ln \sigma / \mathrm{d} \ln \dot{\epsilon}) = 0$ is hereafter referred to as the plateau region. At higher stresses, $m$ has a maximum value of about 0.3 to 0.4 and then decreases with increasing stress. This latter region will be referred to as region II. These two regions are marked on Fig. 9. Region II is the region of superplastic deformation (maximum in $m$). Because of the limitation of recording speed in the equipment used, higher relaxation rates than those shown could not be studied. Therefore, the data do not extend appreciably into the high stress engineering creep range. If the present data are compared to results from earlier studies [14–16] where the strain-rate change technique was employed to measure $\dot{\epsilon}$–$\sigma$ relationships, there is good agreement in region II (taking $K_{\text{total}} = 1.13 \times 10^6 \mathrm{N\,m^{-1}}$). The earlier studies do not extend into the plateau region and hence a comparison at low strain-rates is not possible.

The grain size dependence of the deformation rate was obtained from the data in Fig. 9. Values of $\mathrm{d}P/\mathrm{d}t$ were taken for different grain sizes at stresses of $6.9 \times 10^6$ and $3.4 \times 10^6 \mathrm{N\,m^{-2}}$ in region

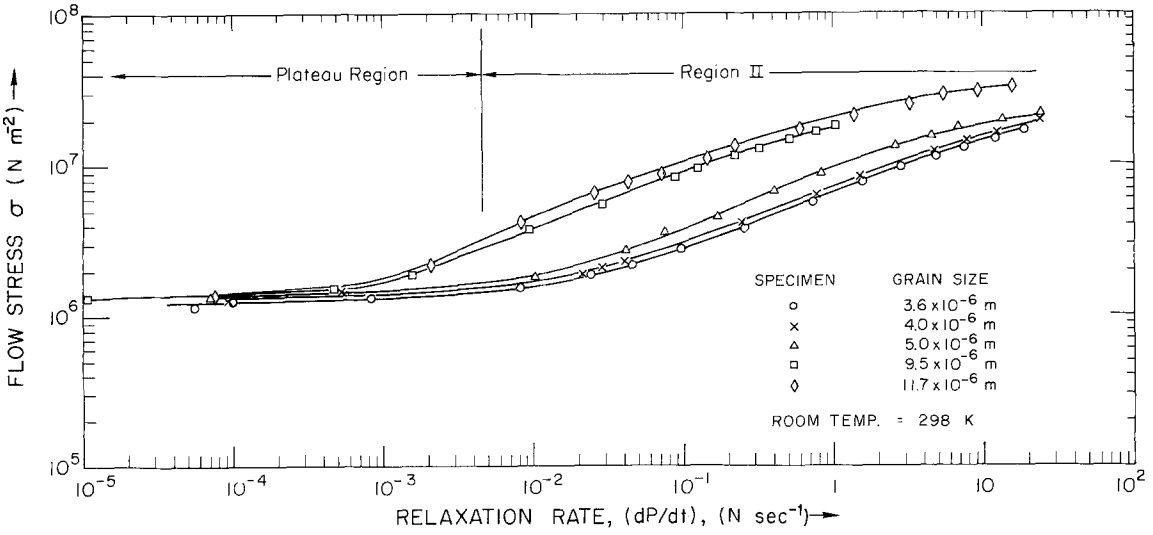


*Figure 9* Variation of relaxation rate with flow stress and grain size for the Pb–Sn eutectic. Division of relaxation rate by $4.3 \times 10^{-4}$N gives approximate strain-rate.

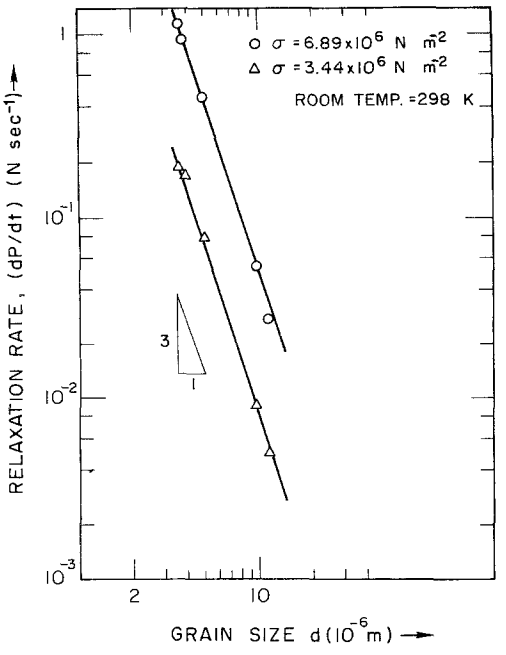


*Figure 10* Grain size dependence of the relaxation rate (deformation rate) for superplastic flow of the Pb–Sn eutectic. Division of relaxation rate by $4.3 \times 10^{-4}$ N gives approximate strain-rate.

II. The corresponding log ($dP/dt$) versus log ($d$) plot is given in Fig. 10. The data show a relationship of $dP/dt \propto d^{-3}$ or $\dot{\epsilon} \propto d^{-3}$ for region II. This relationship is consistent with the analysis of Packer and Sherby [17] for the Pb–Sn eutectic and the results of Alden [18] for Sn–5% Bi. However, the present trend differs somewhat from that observed by Avery and Backofen [14] for the Pb–Sn eutectic, although there is some uncertainty in their $\dot{\epsilon} \propto d^{-2}$ relation as discussed earlier [17]. There appears to be no effect of grain size on the stress level in the plateau region.

To investigate the temperature dependence of the strain-rate, stress relaxation tests were carried out at different test temperatures. The results of these tests are shown in Fig. 11. The data are plotted in accordance with the Arrhenius relationship to determine the activation energy in Fig. 12. In the superplastic region (region II) the activation energy is apparently temperature dependent. This

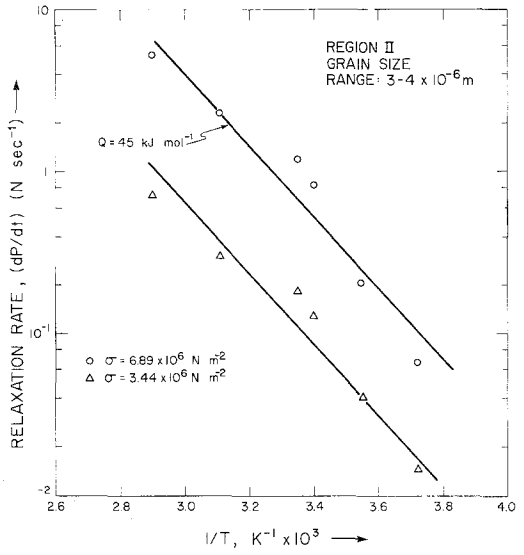


*Figure 12* Activation energy for superplastic flow of the Pb–Sn eutectic. Division of relaxation rate by $4.3 \times 10^{-4}$ N gives approximate strain-rate.

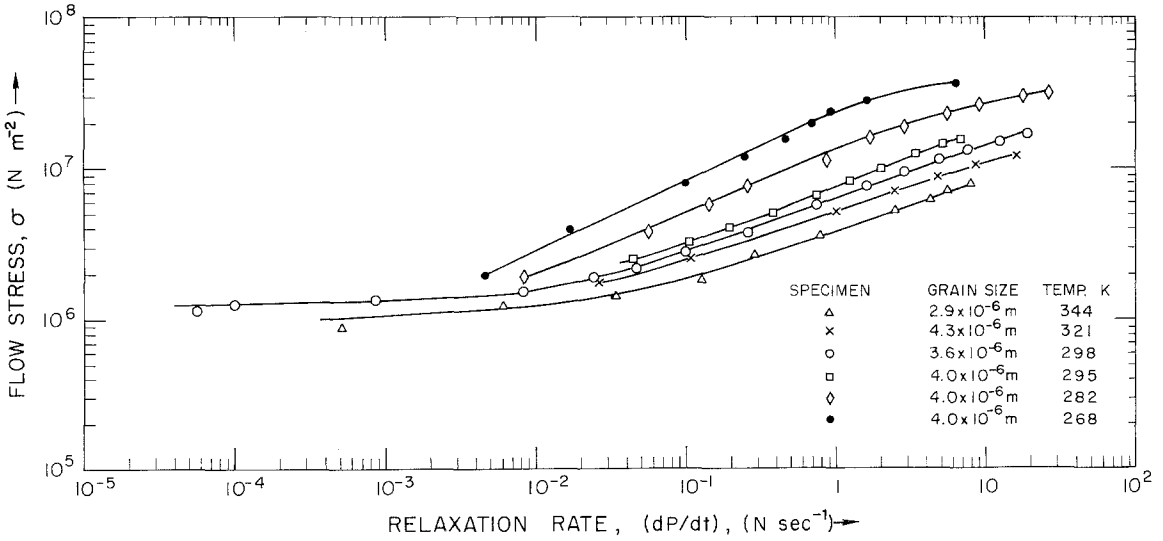


*Figure 11* Influence of test temperature on the stress relaxation behaviour of the Pb–Sn eutectic. Division of relaxation rate by $4.3 \times 10^{-4}$ N given approximate strain-rate.

is perhaps not surprising considering the variable phase composition with temperature and also the fact that the stress dependence of the strain-rate is not constant at constant stress but changes with temperature (see Fig. 11). If we treat the data in Fig. 12 as indicative of a single thermally activated process an average activation energy of $45 \pm 5\ \mathrm{kJ\ mol^{-1}}$ is observed for the entire temperature range investigated.

TABLE I Measured activation energies for superplastic flow in the Pb–Sn eutectic

| Activation energy ($\mathrm{kJ\ mol^{-1}}$) | Reference |
|---|---|
| 46 | Cline and Alden [16] |
| 48 | Baudelet and Suery [19] |
| 46–75 | Avery and Stuarts [20] |
| 32 & 50 | Aldrich and Avery [21] |
| 45 ± 5 | Present work |

TABLE II Bulk ($Q_L$) and grain boundary ($Q_B$) activation energies for Sn and Pb diffusion

| | Activation energy ($\mathrm{kJ\ mol^{-1}}$) | |
|---|---|---|
| | Sn | Pb |
| $Q_L$ | 95.4 [22] | 108 [24] |
| $Q_B$ | 39.9 [23] | 65.7 [25] |
| | | 20.6 [26] |

Tables I and II compare the present data with measured values of diffusion activation energies and activation energies for superplastic flow for this alloy. The $45\ \mathrm{kJ\ mol^{-1}}$ activation energy is in good agreement with previous studies on the superplastic deformation of this alloy and considerably below the lattice diffusion activation energies for pure Sn and Pb. There is reasonable agreement, however, between the grain-boundary diffusion activation energies and the activation energy for superplastic flow.

The significant features of the deformation kinetics to be considered are the presence of the threshold stress (plateau region) and the stress dependence of the deformation rate in the superplastic region. The threshold stress, $\sigma_0$, for superplastic flow can be related to the rate controlling deformation mechanism in the following manner. We assume the dominant deformation process operative in region II, the superplastic region, is grain-boundary sliding with localized accommodation strain or local grain deformation necessary to maintain grain coherency. This deformation mode requires an increase in grain-boundary area as the grains slide past one another [7, 8]. As the applied stress must supply the work to form the new boundary area, there is a threshold stress below which plastic flow by grain-boundary sliding cannot occur. Estimates of the magnitude of this threshold stress $\sigma_0$ appear in the literature [7, 8]. In these treatments $\sigma_0 \propto \gamma/d$ where $\gamma$ is the grain-boundary surface energy and the proportionality constant depends on the exact model. The value of the proportionality constant ranges from about 1 to 10. For the Pb–Sn eutectic $\gamma \simeq 0.25\ \mathrm{J\ m^{-2}}$ and for $d = 3 \times 10^{-6}\ \mathrm{m}$ we have $\sigma_0 \simeq 0.08$ to $0.8 \times 10^6\ \mathrm{N\ m^{-2}}$. These values are somewhat lower than the observed threshold stress of $1.3 \times 10^6\ \mathrm{N\ m^{-2}}$ but not far off at the high end. In apparent disagreement with existing theory, there is no observed grain-size dependence of $\sigma_0$ as observed previously [10]. Burton [11] has also observed a threshold stress for flow in the Pb–Sn eutectic system, but his value of $\sigma_0 = 0.18 \times 10^6\ \mathrm{N\ m^{-2}}$ for $d = 6 \times 10^{-6}\ \mathrm{m}$ is considerably below the present value. The reason for this discrepancy is not known, although Burton's observed plateau region (in terms of strain-rates) is much below (about 100 times) that observed in the present study. Notwithstanding these discrepancies, the presence of the threshold stress is considered to be evidence that there is a minimum stress level necessary for grain-boundary sliding and that this feature should be incorporated in models of superplastic flow [7].

The final feature of the present data to receive comment is the value of the strain-rate sensitivity in the superplastic region (region II). If the grain-boundary sliding is controlled by a grain-boundary diffusion accommodation process then the stress dependence of the strain-rate should go as $\dot{\epsilon} \propto (\sigma - \sigma_0)$. This means that when $\sigma/\sigma_0 \gg 1$ the strain-rate sensitivity $m \to 1$ whereas when $\sigma/\sigma_0 = 1, m \to 0$. The present data do not show $m = 1$ even when $\sigma/\sigma_0 \gg 1$. This is consistent with most other data on superplastic flow where the maximum value of $m \simeq 1/2$. The fact that $\dot{\epsilon} \propto \sigma^2$ is commonly observed over a wide range of $\dot{\epsilon}$ (two decades in some instances [27]) seems to preclude the possibility that $m$ would reach unity as the stress is increased but is prevented from doing so by the onset of recovery-work-hardening creep. This suggests that the superplastic deformation mechanism is not a simple stress driven diffusion process which leads to Newtonian viscosity in the absence of a threshold stress. Rather the deformation mechanism must involve local stress concentrations or some other feature which increases the stress dependence of the deformation rate [28, 29]. This feature of

superplastic flow remains as the major stumbling block to a complete physical understanding of the microscopic processes which accompany superplasticity.

## 4. Conclusions

Dynamic observations of grain-boundary sliding during superplastic flow of the Pb–Sn eutectic alloy coupled with stress relaxation tests have yielded the following information concerning the superplastic flow of this alloy.

(1) During superplastic flow the dominant deformation mode is grain-boundary sliding with some local grain deformation to maintain grain coherency.

(2) Extensive grain-boundary sliding is also observed when the strain-rate and/or grain size is outside the superplastic flow regime. In this instance, however, there is insufficient grain deformation to avoid the formation of cracks and early failure results.

(3) The presence of a finely dispersed precipitate ($AuSn_4$) in the Pb–Sn eutectic does not appreciably alter the superplastic flow mechanism.

(4) The activation energy for superplastic flow was found to be about $45 \pm \text{kJ mol}^{-1}$ and the strain-rate was proportional to the inverse cube of the grain diameter.

(5) A threshold stress for superplastic flow was observed which was independent of grain size in the range 3 to $10 \times 10^{-6}$ m and equal to about $1.3 \times 10^{6}\,\text{N m}^{-2}$.


## Acknowledgements

This work was supported by the United States Atomic Energy Commission under contract No. AT (04–3) 326 PA-17.


## References


1. C. J. DAVIES, J. W. EDINGTON, C. P. CUTLER and K. PADMANABHAN, *J. Mater. Sci.* **5** (1970) 1091.
2. R. H. JOHNSON, *Met. Rev.* **15** (1970) 115.
3. R. B. NICHOLSON, Proceedings of the International Materials Symposium University of California (1972).
4. R. C. GIFKINS, University of Melbourne C.S.I.R.C. Report No. 2 (1971).
5. D. J. DINGLEY, Proceedings of the 3rd Scanning Electron Microscope Symposium (1970) p. 331.
6. E. GECKINLI, C. BARRETT and L. ANDERSON, Proceedings of the 29th EMSA Meeting (1971) p. 11.
7. M. F. ASHBY and R. A. VERRALL, *Acta. Met.* **21** (1973) 149.
8. C. R. BARRETT, Proceedings of the 3rd Nordic High Temperature Symposium, Risø (1972) p. 80.
9. W. A. BACKOFEN, G. S. MURTY and S. W. ZEHR, *Trans. Met. Soc. AIME* **242** (1968) 329.
10. A. KARIM and W. A. BACKOFEN, *Mat. Sic. Eng.* **3** (1968) 306.
11. B. BURTON, *Scripta Met.* **5** (1971) 669.
12. D. LEE and E. W. HART, *Met. Trans.* **2** (1971) 1245.
13. A. BALL and M. HUTCHINSON, *Met. Sci. J.* **3** (1969) 1.
14. D. H. AVERY and W. A. BACKOFEN, *Trans. ASM* **58** (1965) 551.
15. S. W. ZEHR and W. A. BACKOFEN, *ibid* **61** (1968) 300.
16. H. E. CLINE and T. H. ALDEN, *Trans. Met. Soc. AIME* **239** (1967) 710.
17. C. M. PACKER and O. D. SHERBY, *Trans. ASM* **60** (1967) 21.
18. T. H. ALDEN, *Acta Met.* **15** (1967) 469.
19. B. BAUDELET and M. SUERY, *J. Mater. Sci.* **7** (1972) 512.
20. D. H. AVERY and J. M. STUART, Sagamore Army Materials Research Conference "Surface and Interfaces II", Edited by M. Burke, W. Reed and R. Weiss (Syracuse University Press, New York, 1968) p. 371.
21. J. W. ALDRICH and D. H. AVERY, Second International Conference on the Strength of Metals and Alloys. Pacific Grove, California, Vol. III (1970) p. 1094.
22. W. LANGE, A. HASSNER and I. BERTHOLD, *Phys. Stat. Sol.* **1** (1961) 50.
23. W. LANGE and D. BERGNER, *Phys. Stat. Sol. 2* (1962) 1410.
24. H. A. RESING and N. H. NACHTRIEB, *J. Phys. Chem. Solids* **21** (1961) 40.
25. B. OKKERSE, *Acta Met.* **2** (1954) 551.
26. J. P. STARK and W. R. UPTHEGROVE, *Trans. ASM* **59** (1966) 486.
27. J. E. BIRD, A. K. MUKHERJEE and J. E. DORN, "Quantitative Relation Between Properties and Microstructure" (Israel University Press, 1969) p. 255.
28. A. BALL and M. M. HUTCHINSON *Met. Sci. J* **3** (1969) 3.
29. A. K. MUKHERJEE, *Mat. Sci. Eng.* **8** (1971) 83.



Received 21 March and accepted 8 September 1975.